Attosecond Chemical Dynamics

In Progress, Since May 2017

Dr. Atanu Bhattacharya, Assistant Professor
Department of Inorganic and Physical Chemistry
Indian Institute of Science, Bangalore 560012

Preface

.

Table of Contents

Chapter 1: Introduction

Highlights: Born-Oppenheimer Approximation, Koopmans Theorem,

Understanding quantum chemical dynamics has been one of the important goals in physical chemistry. Traditionally chemical dynamics is described based on two simplified description of the interaction between electrons and nuclei.[15,16] One of them includes the adiabatic Born–Oppenheimer approximation.[15] As the nucleus is much heavier than the electron, the electronic configuration is assumed to adapt instantaneously to the nuclear motion. The intrinsic time scale of nuclear motion is femtosecond (1 fs = $1x10^{-15}$ second): origin of this time scale can be easily understood when we analyse the H–H bond vibration (4400 cm^{-1}), for example. The H–H bond vibration exhibits a period of 7.5 fs. Pure electronic motion, however, occurs on attosecond (1 as = $1x10^{-18}$ second) time scale: origin of this time scale comes from a classical picture an electron in its ground state orbiting a hydrogen nucleus. The orbit time can be easily calculated as ~150 as (from Bohr atomic model). Therefore, if the chemistry is driven under the adiabatic Born–Oppenheimer approximation, one may easily conclude that electrons do not play a direct role in chemical dynamics. This is why attosecond time scale may not be important in Born–Oppenheimer chemical dynamics. Figure 1 exhibits situation when Born-Oppenheimer approximation is valid. Under this approximation, total wave function is expressed not as a linear combination of different electronic states; rather, only a single electronic state is involved.

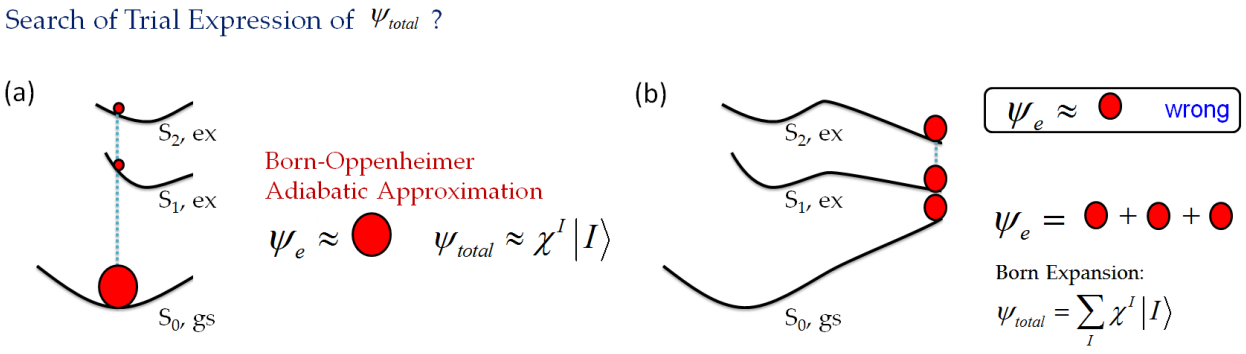

Figure 1: Total wave function under the Born-Oppenheimer approximation and Born Expansion

The adiabatic Born−Oppenheimer approximation breaks down when the energy gap between the adiabatic electronic states is reduced, rendering a situation when electronic motion starts playing an important role in the overall reactivity of the chemical system (see Figure 1(b)). Recent research on photochemistry and photophysics evidences that the electronic motion cannot be neglected in photochemistry and photophysics of polyatomic molecules, particularly when the process involves the conical intersection.[17,18] Conical intersections are regions in the multidimensional potential energy landscape where two electronic adiabatic states become degenerate and where the Born−Oppenheimer approximation completely breaks down. However, we must note that conical intersections are the regions where the electron dynamics slows down from its natural time scale (attosecond) to the time scale of nuclear motion (femtosecond).19 Therefore, electronic motion can be important in conical intersection-mediated non-Born−Oppenheimer chemical dynamics but the attosecond time scale may not be important in the same.

Another approximation, which is frequently used to describe chemical dynamics, is the one-electron approximation (or mean field approximation).[16] Under this approximation, one electron is considered to be individual particle moving under the influence of an average (or mean) field generated by all other electrons. The Hartree−Fock (HF) theory was developed under this approximation.[16] The HF theory, for the first time, give us the concept of molecular orbital: the Eigen function of one electron Fock operator. Another interesting definition of molecule orbital from HF theory emerges on the basis of the interpretation given by Koopmans:[20] the first ionization energy of a molecular system is equal to the negative of the energy of the highest occupied molecule orbital (HOMO) under the closed-shell HF theory. Similar Koopmans definition of molecular orbital is also valid at the Density Functional Theory (DFT); however, more precise definition of molecular orbitals at the DFT comes from Kohn-Sham orbitals which are defined as the Eigen function of Kohn-Sham one electron equation.

Koopmans theorem is valid only if the orbitals of the cation are identical to those of the neutral molecule (frequently called frozen orbital approximation). This theorem becomes invalid under two circumstances: (1) orbital relaxation following vertical ionization, if there is a change in the HF or KS orbitals due to change of mean field; (2) electron correlation following ionization, if HF or KS wave function (single Slater determinant wave function) fails to represent the entire many-body wave function (in that case, a multiconfiguration wavefunction is necessary to represent the post-ionization event). Recent literature shows that several important and perhaps hitherto- unknown pure electronic processes can occur in attosecond time scale when Koopmans theorem breaks down.[10−13] Therefore, the attosecond time scale becomes important in chemistry when an ionization process is involved and when Koopmans theorem breaks down.

Currently attosecond chemical dynamics is an emerging field of research. Perhaps, everybody working in the field of attosecond chemical dynamics would agree that it is difficult to introduce this subject to a new student with a chemistry background. The reason is not chemistry students' lower intellectual level; rather, the reason is that chemists' mind is preoccupied by the picture of chemical bonding which invokes frozen molecular orbitals (e.g. MO theory) to describe the reactivity and chemical dynamics. Hence, an article of chemical education describing the role of attosecond time scales in the chemical dynamics is very timely and appropriate. This article is written with this intention only.

Vertical Ionization and Superposition of Molecular Orbitals:

To begin the discussion of vertical ionization and associated attosecond electron dynamics, we shall look at the KS orbitals of NCCl:NH_3 complex. At the neutral ground state, this complex exhibits a non-covalent bonding interaction between Cl and N atoms (see ref. # for more detailed discussion). More specifically this interaction is called halogen bonding interaction. The KS-HOMO of this neutral species computed at the wB97XD/6-31G(d) level of theory (under the restricted-SCF scheme) is shown in Figure 2.

Now, if an electron is removed from the KS-HOMO, the mean field experienced by each electron in the system is changed because of the newly created positive charge in the electronic cloud. This newly emerged mean field can be optimized with the help of self-consistent field (SCF) calculation. In Gaussian09, convergence of SCF calculation is controlled with the help of an option "Conver=N". This option sets the SCF convergence criterion to 10^{-N}. The SCF convergence requires both $<10^{-N}$ RMS change in the density matrix and $<10^{-(N-2)}$ maximum change in the density matrix. Here we note that the energy change is not used to test the SCF convergence; however, an SCF 10^{-N} RMS density matrix change typically corresponds to a 10^{-2N} change in energy in atomic units.

Figure 2 depicts neutral HOMO of NCCl:NH_3 complex. This HOMO exhibits electron density mostly localized on NH_3-end of the complex. When we attempt of optimize the positive charge in the ground cationic surface of NCCl:NH3 system, we find that nature of and The time-dependent quantum chemistry teaches us that solution (using variable separation method) of the time-dependent Schrodinger equation for a pure state (also called stationary state,

characterized by its own characteristic time-dependent phase factor) depends on time: $\psi(x,t) = \psi(x) \exp(-iEt/\hbar)$. However, the probability density of this pure state is independent of time. This probability density is closely related to what we observe in the experiment. We obtain time dependence in the probability density only when a state (more specifically a nonstationary state) is prepared via linear combination (coherent superposition) of stationary (pure) states, each with its own characteristic time-dependent phase factor. Considering linear combination of two pure states, for example, the probability density of the nonstationary state is given by

Equation 2 has three terms: the first and second ones come frompure $\psi1(x,t)$ and $\psi2(x,t)$, and the third one comes from an (oscillatory) interference term. This interference term is a result of having a superposition of eigenstates with different energiescalled a wavepacket. All the time-evolving features of the nonstationary state $\psi(x,t)$ are buried inside this interference term. For an example, time dependence of the probability density of this nonstationary state can be simply expressed by its characteristic oscillation period, $\tau = h/\Delta E$, where the oscillation frequency is given by $\upsilon = \Delta E/h$. With the basic idea presented above, we now ask what happens when one removes an electron from a particular molecular orbital (following vertical ionization)? Under one electron approximation, a localized hole is created at the HOMO, if the electron is removed from the HOMO. The HOMO of the neutral molecule or cluster may not be a stationary orbital of the cation. It can happen that neutral HOMO is a linear combination of several cationic states. In that case, vertical ionization (which is simply manifested by removal of an electron from the HOMO) coherently populates more than one cationic Eigenstates. This creates an electronic wavepacket that evolves in time (according to the law of superposition). The reason for wavepacket generation via the vertical ionization is the electron−electron relaxation and correlation. Without electron−electron relaxation and correlation, the vertical ionization prepares only a pure cationicstate and, as a result, the hole density of a pure state does notevolve in time.

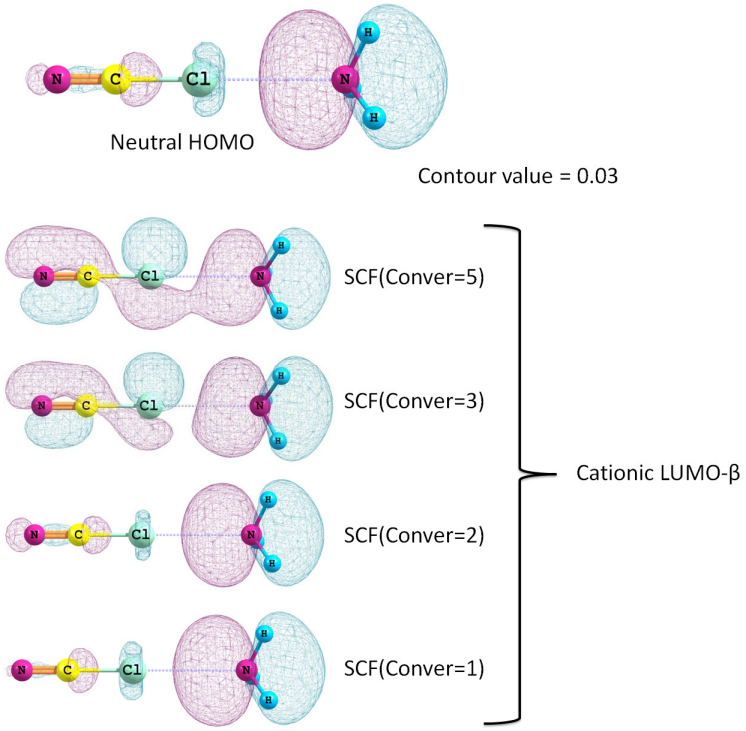

About a decade ago, Levine and Remacle proposed a simple procedure to investigate the time evolution of a non-stationary electronic state prepared via the vertical ionization.13 After removal of an electron from the HOMO of the neutral (featuring the vertical ionization) a localized hole is created in the neutral HOMO. Under the unrestricted self-consistent field (SCF)scheme, the neutral HOMO can be expressed as a linear combination of all cationic orbitals and projections (determined by overlap integrals) of the neutral HOMO onto both the α- and the β-cationic orbitals can be taken as expansion coefficients.

Finally, the time evolution of the hole orbital associated with two spins can be represented by introducing the time-dependent phase factor (see Supporting Information S3 for more details):

Here, ΨHOMO is the HOMO of the neutral cluster, Φλ is the λth cationic MO of the cluster, $|\Psi\alpha(0)\rangle$ and $|\Psi\beta(0)\rangle$ are the hole orbitals with spin labels α and β, respectively.

Ultrafast charge migration dynamics in ionized halogen-, chalcogen-, pnicogen-, and tetrel-bonded clusters was studied using eqs 3 and 4. Figure 1 (and Supporting Information S4) shows the hole migration dynamics through the Cl···N halogen, S···N chalcogen, P···N pnicogen, and Si···N tetrel noncovalent bonds for selected (1:1) complexes (H_2NCl:NH_3, H_2NSH:NH_3, H_2NPH_2:NH_3, and H_2NSiH_3:NH_3, respectively), computed at the DFT level of theory (with wB97XD functional and 6-31+G(d,p) basis set). Comparison of different levels of theory (DFT vs CASSCF) was made earlier.35−37 Figure 1 shows that atthe moment of ionization, the hole density is purely localized on the H2NX end; however, this hole density rapidly gets delocalized over the respective noncovalent bond in approximately 400−500 attosecond. A similar time scale is also predicted for many other halogen-,chalcogen-, pnicogen-, and tetrel-bonded clusters. 35−37

Analytical Theory:

Let us consider an isolated molecular system in its electronic and vibrational ground state before ionization. Vertical ionization with an ideal VUV monochromatic photon renders an electronic cationic state. If

The initial hole orbital (immediately after the vertical ionization) can be expressed as a linear combination of the two cationic molecular orbitals,

$$\psi_h(r,t=0;R_0)=\left[c_{0+}\psi_{0+}(r;R_0)+c_{1+}\psi_{1+}(r;R_0)\right] \quad \text{..... (1)}$$

Here, the expansion coefficients in the adiabatic basis are assumed to be independent of the geometry R for simplicity. The hole orbital at any time t can be obtained by

$$\psi_h(r,t=0;R_0)=\left[c_{0+}e^{\frac{-iE_{0+}t}{\hbar}}\psi_{0+}(r;R_0)+c_{1+}e^{\frac{-iE_{1+}t}{\hbar}}\psi_{1+}(r;R_0)\right] \quad \text{..... (2)}$$

This definition of hole orbital is valid for fixed equilibrium geometry (R_0). At the fixed nuclear geometry (equilibrium) time dependent hole density is then expressed as,

$$\rho(r,t;R_0) = \left|\psi_h(r,t=0;R_0)\right|^2$$
$$= \left[\left|c_{0+}\right|^2 \left|\psi_{0+}(r;R_0)\right|^2 + \left|c_{1+}\right|^2 \left|\psi_{1+}(r;R_0)\right|^2 + c_{0+}c_{1+}^* e^{\frac{-i(E_{0+}-E_{1+})t}{\hbar}} \psi_{0+}(r;R_0)\psi_{1+}^*(r;R_0) + c.c. \right] \quad \text{..... (3)}$$

or,

$$\mathrm{Re}\left[\rho(r,t;R_0)\right]$$
$$= \left[\left|c_{0+}\right|^2 \rho_{00}(r;R) + \left|c_{1+}\right|^2 \rho_{11}(r;R) + 2c_{0+}c_{1+}^* \cos\left(\frac{\Delta E(R_0)t}{\hbar}\right)\rho_{01}(r;R) \right] \quad \text{..... (4)}$$

Equation (4) is obtained assuming real initial expansion coefficient and real basis states. This equation manifests that the hole density would oscillate at a well-defined frequency determined by $\frac{\Delta E(R_0)}{\hbar}$. However, spatial delocalization of the nuclear wave packet of the neutral species is an unavoidable initial condition of the vertical ionization process. What does it mean? See Figure 1. Experimentally, when we ionize a molecule, it is not possible to ionize the molecule at its equilibrium frozen geometry (R_0). Therefore, effect of the width of the nuclear wavepacket has also to be included in equation (1).

Considering any nuclear coordinate the hole orbital can be expressed as

$$\psi_h(r,t=0,R) = g(R)\left[c_{0+}e^{\frac{-iE_{0+}t}{\hbar}} \psi_{0+}(r;R) + c_{1+}e^{\frac{-iE_{1+}t}{\hbar}} \psi_{1+}(r;R) \right] \quad \text{..... (5)}$$

Thus, time dependent hole density can be expressed as

$$\mathrm{Re}\left[\rho(r,t,R)\right]$$
$$= \left|g(R)\right|^2 \left[\left|c_{0+}\right|^2 \rho_{00}(r;R) + \left|c_{1+}\right|^2 \rho_{11}(r;R) + 2c_{0+}c_{1+}^* \cos\left(\frac{\Delta E(R)t}{\hbar}\right)\rho_{01}(r;R) \right] \quad \text{..... (6)}$$

As the oscillatory term (the sum of the off-diagonal elements of the electron density matrix, which determines electronic coherences) determines time dependent change of the hole density, we shall now focus only on this term:

$$c(r,t,R) = \left|g(R)\right|^2 2c_{0+}c_{1+}^* \cos\left(\frac{\Delta E(R)t}{\hbar}\right)\rho_{01}(r;R) \quad \text{..... (7)}$$

The effect of the spatial delocalization of the nuclei can be taken into account by calculating the expectation value of $c(r,t,R)$ over the range of nuclear geometries:

$$\left\langle c(r,t,R)\right\rangle = 2c_{0+}c_{1+}^{*}\int_{-\infty}^{+\infty}\left|g(R)\right|^{2}\cos\left(\frac{\Delta E(R)t}{\hbar}\right)\rho_{01}(r;R)dR \quad \text{..... (8)}$$

To obtain a solution, we shall assume that $\rho_{01}(r;R)$ does not change much with R and it can be approximated to the constant, $\rho_{01}(r;R_0)$. Then the equation (8) reads

$$\left\langle c(r,t,R)\right\rangle \simeq 2c_{0+}c_{1+}^{*}\rho_{01}(r;R_0)\int_{-\infty}^{+\infty}\left|g(R)\right|^{2}\cos\left(\frac{\Delta E(R)t}{\hbar}\right)dR \quad \text{..... (9)}$$

Under the harmonic approximation, the vibrational ground state wave function can be expressed as (normalized Gaussian):

$$g(R)=\left(\frac{2\beta}{\pi}\right)^{1/4}e^{-\beta(R-R_0)^2} \quad \text{..... (10)}$$

where, $\beta=\frac{\alpha}{2}$, this β parameter determines the width of the Gaussian $\left(\Delta R=2\sqrt{\frac{\ln 2}{\beta}}\right)$; R_0 determines the center of the Gaussian (which features the position of equilibrium geometry of the neutral species). See Figure 1 for the pictorial depiction of such Gaussian. Inserting equation (10) into equation (9), we get

$$\left\langle c(r,t,R)\right\rangle \simeq 2c_{0+}c_{1+}^{*}\rho_{01}(r;R_0)\left(\frac{2\beta}{\pi}\right)^{1/2}\int_{-\infty}^{+\infty}e^{-2\beta(R-R_0)^2}\cos\left(\frac{\Delta E(R)t}{\hbar}\right)dR \quad \text{..... (11)}$$

If we consider, for simplicity, a linear variation of the cationic molecular orbital energies, as depicted in Figure 2, we can write $\Delta E(R)=\left|R\right|d$, where R and d represents inter nuclear coordinate and gradient difference between two lines. Insertion of this relationship into equation (11) helps us integrate the equation. After integration we get

$$\left\langle c(r,t,R)\right\rangle \simeq 2c_{0+}c_{1+}^{*}\rho_{01}(r;R_0)e^{\frac{-d^2t^2}{8\hbar^2\beta}}\cos\left(\frac{\Delta E(R)t}{\hbar}\right) \quad \text{..... (12)}$$

Equation (12) suggests that the cosine oscillation of the equilibrium geometry obtained at $R=R_0$ diminishes with time by a Gaussian function. As $t\to\infty$, the electronic coherences

disappear: $\langle c \rangle \to 0$. The system decoheres. The origin of the decoherence is not he coupling with an environment but rather dephasing due to initial wavepacket width.

The time at which the amplitude of the cosine oscillation is reduced to half its initial value due to Gaussian decay is given by

$$t_{1/2} \sim \frac{2\sqrt{2\beta\hbar^2 \ln 2}}{d} \quad \text{..... (13)}$$

Thus, coherence half life depends on two physical properties of the system: It would be long if (a) the wavepacket is narrow (large β); and (b) gradient difference between two cationic molecular orbital curves is small (if these curves are almost parallel). Both characteristics result in a narrow energy-gap distribution which postpones the dephasing. The position of the equilibrium geometry of the neural species does not affect $t_{1/2}$; it only determines the period of the oscillation.

The above simple analytical model shows the origin of attochemistry due to vertical ionization process. In addition, it shows that how the nuclear wavepacket width leads to the dephasing of the electron dynamics oscillations. However, there are several limitations: the nuclei are kept fixed (the kinetic operator of the nuclei is absent from the Hamiltonian of the system) and the interaction between the cation and the photoelectron is not taken into account (assuming a photoelectron with high kinetic energy and therefore, ionization by a high energy photon). Finally, the electron density is calculated as an expectation value over all nuclear geometries treated independently.

Our next motivation should be to investigate numerically the decoherence of electron dynamics in real molecular system. In particular we are interested in noncovalent bonded systems using density functional theory (DFT).

Density Functional Theory:

Consider a system of N electrons that do not interact at all. They are subjected to external potential $V_0(r)$ (source of external potential could be Coulombic interaction with the nuclei), so intelligently tailored, that ρ does not change; i.e., we still have ideal ground state electron density, $\rho = \rho_0$. Then Kohn-Sham one electron equation reads

$$\left[-\frac{1}{2}\Delta + V_0(r)\right]\varphi_i = \varepsilon_i \varphi_i$$

Here, φ_i is some spin-orbital, called the Kohn-Sham orbital. The total wave function is a Slater determinant (more specifically the Kohn-Sham determinant: antisymmetrized product of spin orbital). Electronic density distribution of such system is given by

$$\rho(r) = \sum_i n_i \left|\varphi_i\right|^2$$

We note that $\rho(r)$ can be exact (100% correlated) if $V_0(r)$ operator can be guessed exactly. Thus the electronic ground-state energy of the system can be written as

$$E = T_0 + \int V(r)\rho(r)dr + J(\rho) + E_{xc}(\rho)$$

Here, T_0 is the electronic kinetic energy of the fictitious Kohn-Sham system of non-interacting electrons. $\int V(r)\rho(r)dr$ represents the correct electron-nuclei interaction (or other external potential term). $J(\rho)$ features self-interaction term (an interaction of the electron cloud with itself):

$$J(\rho) = \frac{1}{2}\iint \frac{\rho(r_1)\rho(r_2)}{\left|r_1 - r_2\right|} dr_1 dr_2$$

This expression contains conceptually wrong component: for one electron system (e.g., H atom) this expression exhibits an inter-electronic self-repulsion which actually does not exist because we have only one electron. The same problem exists even for multielectron system and this is why $J(\rho)$ needs to be corrected for self-interaction error.

Finally, $E_{xc}(\rho)$, which is called exchange correlation energy, represents everything which includes lacking reminder. This may be a strange definition but $E_{xc}(\rho)$ includes exchange and correlation effects as well as a correction to the kinetic energy term that takes into account that kinetic energy has to be calculated for interacting electrons. However, what is the mathematical form of $E_{xc}(\rho)$? This is a good question. No ab initio method exists to make this guess. We have to just predict.

Thus, Kohn-Sham equation finally reads

$$\left[-\frac{1}{2}\Delta + V + V_{coul} + V_{xc}\right]\varphi_i = \varepsilon_i \varphi_i$$

Here, V represents electron cloud-nuclear interaction, V_{coul} is self-interaction, V_{xc} is exchange correlation interaction. This equation is analogous to the Fock equation. The Kohn-Sham equation can be solved by an iterative method (self-consistency is achieved).

Figure 1: Two Sides of Vertical Ionization: (a) Molecule is electronically excited from neutral ground state to the cationic state (here cationic ground state is considered for an example) and (b)

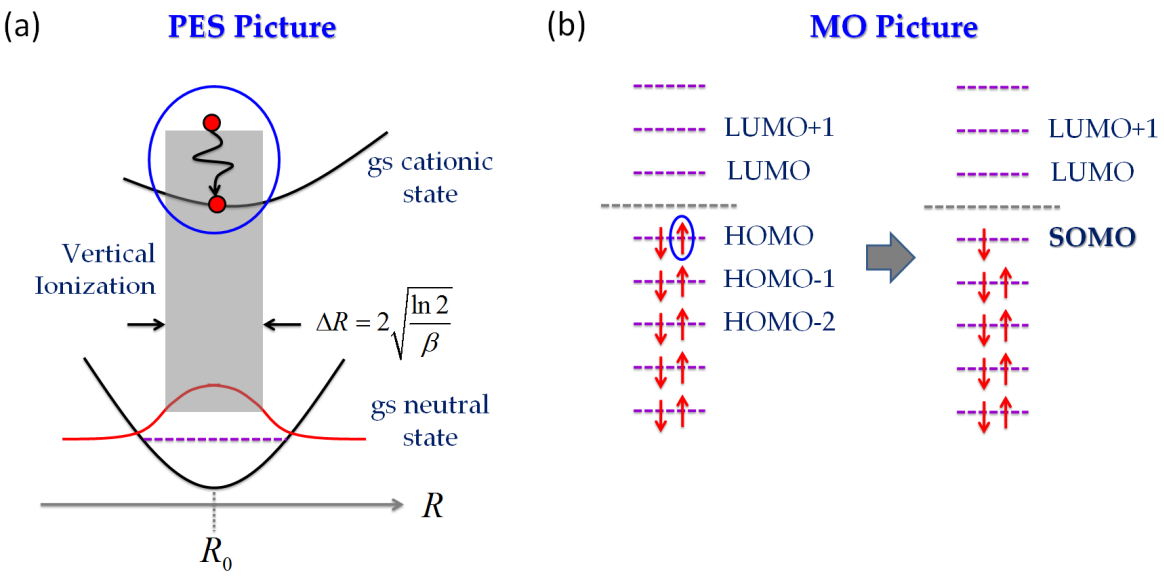

Figure 2: A linear variation of the cationic molecular orbitals, which are involved in the superposition, is assumed for simplicity. This assumption enables us to find a relationship between energy gap and gradient difference between two lines. Here d represents gradient difference between two lines.

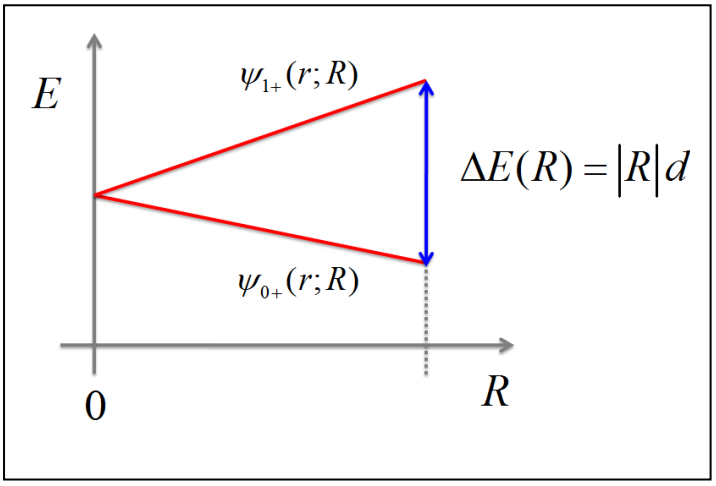

.

Raising Experimental Curiosity:

A few Practical Problems from Physical Chemistry:

1. Thermodynamics: Heat of reaction (ΔH_r) is defined as the amount of energy or heat absorbed or released in a reaction.

To determine the ""heat of reaction" of a reaction experimentally, we need to monitor the

temperature of a reaction over time, using temperature probe (or sensor, e.g., a thermocouple). This experiment is called calorimetry (science of measuring heat). Without a standalone "calorimeter" instrument, how can we perform the measurement and record and plot the data directly in computer hard disk? What are the components required to set-up such measurement?

2. Spectroscopy:

In electronic spectroscopy, we can develop the concept of energy levels (σ, σ^*, π, π^*), interaction of light with molecules, chromophores for $\sigma \rightarrow \sigma^*$ and $\pi \rightarrow \pi^*$ transitions, effect of conjugated double bonds on $\pi \rightarrow \pi^*$ transitions, absorbed color vs. observed color based on the electronic spectra recorded experimentally.#######

Chapter 1: Strong Field Science - Early Door to the Attosecond Science

Highlights: Laser Induced Breakdown, Multiphoton Ionization, Above Threshold Ionization, Tunnel Ionization, High Harmonic Generation

Many fundamental concepts of attosecond science have emerged over the past several decades under the name of strong-field physics and chemistry. This is why a quick review of strong field laser-matter interaction would be useful for the readers new to the field. This chapter presents the progress of the strong field science closely following the personal account recently presented by Chin.[1] The entire development of the strong field physics and chemistry started with laser-induced breakdown of gases, followed by multiphoton ionization and tunnel ionization of atoms and molecules. The development of strong field science is still continuing into the current state of attosecond and ultrafast X-ray science. Our discussion in this chapter, thereby, will begin with the laser induced breakdown of gases observed in the early 1960s. Then multiphoton ionization will be discussed. Finally the concept of tunnel ionization, which is considered to be the first step towards the synthesis of ultrafast X-ray laser, will be discussed.

Laser Induced Breakdown:

Our understanding of strong field science began with laser induced breakdown of gases in the early 1960s. Discovery of the Q-switched ruby laser[2] around 1961 sparked this beginning by creating laser induced plasma in gaseous medium because the Q-switched ruby laser, for the first time, provided the required extremely high intensity of the laser beam for experimentally exploring strong field science. Meyerand and Haught observed a spark in air when the Q-switched ruby laser beam was focused into air.[3] It was recognized that the spark involved the ionization of the air molecules. However, single photon ionization of air molecules was not possible because the ionization potentials of air molecules (O_2=12.1 eV and N_2=15.6 eV) were much higher than laser photon energy of the Q-switched ruby laser (1.79 eV). It was, therefore, realized that multiphoton ionization process must be involved in laser induced breakdown of air. Extensive theoretical and experimental works finally confirmed the involvement of three steps in optical breakdown of gases:[4]

Step 1: Multiphoton Ionization of molecules with low ionization potentials generate a few free electrons with low kinetic energies in the focal volume of the laser-gas interaction region.

Step 2: The free electrons in the strong laser field absorbs photons (say n numbers) while colliding with heavier particles (such as, atoms, molecules, ions). This process is called inverse Bremsstrahlung or free-free transition.

Step 3: The free-free transition forces the free electrons to acquire a kinetic energy higher than the ionization potential of the gas molecules. Collisions of the high energy electrons with high potential energy gas molecules further ionize the gas molecules.

Q-Switching (active and passive):

oscopy

Steps 1-3 are repeated during laser induced breakdown process, resulting in avalanche ionization process or breakdown. The details of laser induced breakdown, particularly free-free transition, fall outside the scope of this book; however, the first step, multiphoton ionization which initiates the laser induced breakdown process, has its own physical interest in the core context of the present book.

Multiphoton Ionization:

Our understanding of strong field science begun with laser induced breakdown of gases in the early 1960s. Discovery

origin of idea

,

References:

1. S. L. Chin, From Multiphoton to Tunnel Ionization, Chapter 3 in Advances in Multi-Photon Processes and Spectroscopy, Eds. S. H. Lin, A. A. Villaeys, Y. Fujimura, vol. 16, World Scientific.
2. F. J. McClung and R. W. Hellwarth, Giant Optical Pulsations from Ruby, *J. Appl. Phys.,* 33, 828 (1962).
3. (a) R. G. Meyerand and A. F. Haught, Gas Breakdown at Optical Frequencies, *Phys. Rev. Lett.*, 11**,** 401 (1963); (b) R. G. Meyerand and A. F. Haught, Optical-Energy Absorption and High-Density Plasma Production, *Phys. Rev. Lett.*, 13, 7 (1964).
4. C. G. Morgan, Laser-induced breakdown of gases, *Rep. Prog. Phys.*, 38, 621 (1975).

Further Reading:

1. S. H. Lin, Y. Fujimura, H. J. Neusser, E. W. Schlag, Multiphoton Spectroscopy of Molecules, Academic Press Inc., New York, 1984.

...

Chapter 2: High Harmonic Generation: Experiments

Highlights:

Introduction:

High harmonic generation (HHG) represents an extreme nonlinear process, in which more than 10 or even 100 input photons from a visible or near infrared (NIR) laser are combined together in a frequency up-conversion process, as depicted in Figure #. HHG provides an attractive source of coherent radiation in the extreme ultraviolet (XUV) and soft X-ray region. Much of the currently on-going experimental works in HHG is revolving around increasing the efficiency of the process.

HHG occurs when an intense laser pulse is focused into a noble gas medium (such as He, Ar, etc.), as depicted in Figure #. The required focused intensity of the fundamental beam for this process is at least 10^{13} w/cm^2 and can be obtained by focusing a high power femtosecond laser beam. At this or higher than this intensity, the contribution of very high order nonlinearity becomes significant.

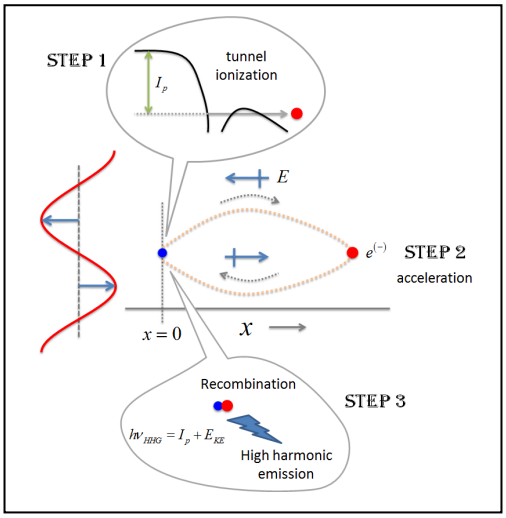

Figure #: Three step classical model for HHG

Although the most accurate description of HHG process involves numerical solution of the non-linear Schrodinger equation, a quasi-classical three step model, proposed by Corkum in 1993 [2], can also accurately predicts the general features of HHG. According this model, as

depicted in Figure #, in the first step, the intense laser field suppresses the columb potential of the atom, allowing tunnel ionization. Second step involves evolution of the "free" electron in the laser field. As the optical field oscillates, it first propels the electron away from the ion and then, when the field reverses, the field accelerates the electron back towards the ion. Finally the third step is recombination of the free electron with its parent ion, emitting high harmonic photon ($h\nu_{HHG} = I_p + E_{KE}$). The ionization and recombination can occur on every half-cycle of the driving field. As HHG occurs in noble gas medium, which features an isotopic medium and has inversion symmetry, the $P-E$ function introduced early in this chapter gets odd symmetry, i.e., $P-E$ function becomes odd function. This means that even terms are all zero and $P-E$ function for HHG becomes

$$P(z,t) = \varepsilon_0\left(\chi^{(1)}E(z,t) + \chi^{(3)}E^3(z,t) + \chi^{(5)}E^5(z,t).....\right)$$

and this is why only odd harmonics are generated.

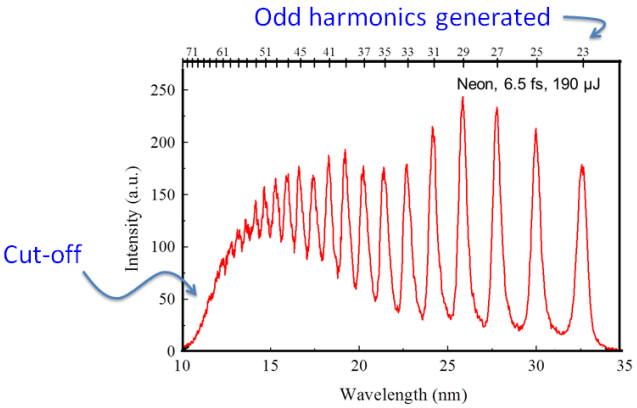

Figure #: Typical HHG spectrum obtained in Ne gas medium

A typical harmonic spectrum is depicted in Figure #, which exhibits generated odd harmonics and a sharp cut-off (above which no harmonics is produced) in the spectrum. The highest possible harmonic photon energy can be given by simple cut-off rule:

$$h\nu_{MAX}^{HHG} = I_P + 3.2U_p,$$

where, $3.2U_p$ is the maximum kinetic energy and U_p is the time-averaged kinetic energy gained by the electron during Step 2. U_p is known as Ponderomotive energy:

$$U_p = \frac{e^2 |a(t)|^2}{4m_e\omega_0^2} = \frac{e^2 I(t)}{4m_e\omega_0^2} = \frac{e^2}{4m_e(4\pi^2 c)} I(t)\lambda_0^2 ; \left[\text{as, } \omega_0 = 2\pi\frac{c}{\lambda_0}\right]$$

Therefore, $U_p \propto I(t)\bullet\lambda_0^2$

According to the above equation, the cut-off can be extended by increasing the Ponderomotive energy U_p, which can be achieved by using longer wavelength of the fundamental laser beam. In addition, based on this equation, extension of the position of the cut-off to higher photon energy is also possible by using atoms with high ionization potential IP, such as He. Now we shall derive cut-off rule using three step model.

Mathematical Formulation of Three Step Model:

Figure # depicts the three step model, which include (1) tunnel ionization, (2) acceleration, and finally (3) recombination. In order to derive mathematical expression for the electron trajectory, Ponderomotive energy and cut-off rule, we shall consider plane waveas input beam. The real field is represented by

$$E(t) = E_0 \cos\omega_0 t$$

Here, we have considered that field does not depend on space coordinate. This is reasonable approximation as long as the wavelength of the input beam is large compared to the atomic size. In addition, a few assumptions are employed:

(1) Electron was at rest in an atom before tunnel ionization.
(2) Electron was suddenly completely free, i.e., electron will face only electric field of the laser. Electric field of the parent ion is ignored.
(3) Electron is accelerated (at time $t = t_0$) from position $x = 0$ along the x axis.

Thus, the force experienced by the electron due to oscillating electric field is given by

$$F = m\frac{\mathrm{dv}}{\mathrm{dt}} = -eE_0 \cos\omega_0 t$$

Integrating both sides with respect to t , we get,

$$\mathrm{v}(t) = \frac{-eE_0}{m\omega_0}\sin(\omega_0 t) + \mathrm{v}_0$$

According to the assumptions made above, electron was at rest at the time of ionization. So at $t = t_0$, v=0. Inserting this initial condition, we get $\mathrm{v}_0 = \frac{eE_0}{m\omega_0}\sin(\omega_0 t_0)$. Thus, equation can be rewritten as

$$\mathrm{v}(t) = \frac{-eE_0}{m\omega_0}\sin(\omega_0 t) + \frac{eE_0}{m\omega_0}\sin(\omega_0 t_0)$$

$$\text{or, } \frac{dx}{dt} = \frac{-eE_0}{m\omega_0}\sin(\omega_0 t) + \frac{eE_0}{m\omega_0}\sin(\omega_0 t_0)$$

Integrating both sides with respect to t, we get

$$x(t) = \frac{eE_0}{m\omega_0^2}\cos(\omega_0 t) + \frac{eE_0 t}{m\omega_0}\sin(\omega_0 t_0) + x_0$$

Again, using the assumption that at $t = t_0$, $x = 0$, we get, $x_0 = \frac{-eE_0}{m\omega_0^2}\cos(\omega_0 t_0) + \frac{-eE_0 t_0}{m\omega_0}\sin(\omega_0 t_0)$. Inserting this in the above equation, we get

$$x(t) = \frac{eE_0}{m\omega_0^2}\cos(\omega_0 t) + \frac{eE_0 t}{m\omega_0}\sin(\omega_0 t_0) - \frac{eE_0}{m\omega_0^2}\cos(\omega_0 t_0) - \frac{eE_0 t_0}{m\omega_0}\sin(\omega_0 t_0)$$

This equation features the oscillatory trajectory of the electron in the input electric field.

It is also assumed that at the time of recombination, the electron comes back to rest. If time taken by electron for acceleration and recombination is defined by τ, then at $t = (t_0 + \tau)$, $x = 0$. Substituting for this final time in the above equation, we get

$$\frac{eE_0}{m\omega_0^2}\cos\left[\omega_0\left(t_0 + \tau\right)\right] + \frac{eE_0\left(t_0 + \tau\right)}{m\omega_0}\sin(\omega_0 t_0) - \frac{eE_0}{m\omega_0^2}\cos(\omega_0 t_0) - \frac{eE_0 t_0}{m\omega_0}\sin(\omega_0 t_0) = 0$$

Using $\cos(A + B) = \cos A\cos B - \sin A\sin B$ identity, we can rewrite the above equation as

$$\cos(\omega_0 t_0)\cos(\omega_0\tau) - \sin(\omega_0 t_0)\sin(\omega_0\tau) + \omega_0 t_0\sin(\omega_0 t_0) + \tau\omega_0\sin(\omega_0 t_0) - \cos(\omega_0 t_0) - t_0\omega_0\sin(\omega_0 t_0) = 0$$

$$\text{or, } \cos(\omega_0 t_0)\cos(\omega_0\tau) - \sin(\omega_0 t_0)\sin(\omega_0\tau) + \tau\sin(\omega_0 t_0) - \cos(\omega_0 t_0) = 0$$

$$\text{or, } \cos(\omega_0 t_0)\left[\cos(\omega_0\tau) - 1\right] - \sin(\omega_0 t_0)\left[\sin(\omega_0\tau) - \tau\omega_0\right] = 0$$

$$\text{or, } \frac{\sin(\omega_0 t_0)}{\cos(\omega_0 t_0)} = \frac{\left[\cos(\omega_0 \tau) - 1\right]}{\left[\sin(\omega_0 \tau) - \tau\omega_0\right]}$$

$$\text{or, } \tan(\omega_0 t_0) = \frac{\left[\cos(\omega_0 \tau) - 1\right]}{\left[\sin(\omega_0 \tau) - \tau\omega_0\right]}$$

Now we shall go back to equation, featuring electron trajectory, to estimate final kinetic energy gained by electron immediately before recombination (i.e., kinetic energy gained due after time $t = (t_0 + \tau)$), which can be written as

$$\begin{aligned}
E_k &= \frac{1}{2}\mathrm{m}v^2(t_0 + \tau) \\
&= \frac{1}{2}\mathrm{m}\left[\frac{eE_0}{m\omega_0}\sin(\omega_0 t_0) - \frac{eE_0}{m\omega_0}\sin(\omega_0 t_0 + \omega_0 \tau)\right]^2 \\
&= \frac{1}{2}\mathrm{m}\frac{e^2E_0^2}{m^2\omega_0^2}\left[\sin(\omega_0 t_0) - \sin(\omega_0 t_0 + \omega_0 \tau)\right]^2 \\
&= \frac{1}{2}\frac{e^2E_0^2}{m\omega_0^2}\left[\sin(\omega_0 t_0) - \sin(\omega_0 t_0)\cos(\omega_0 \tau) - \sin(\omega_0 \tau)\cos(\omega_0 t_0)\right]^2 \\
&= \frac{1}{2}\frac{e^2E_0^2}{m\omega_0^2}\left[\sin(\omega_0 t_0)\left[1 - \cos(\omega_0 \tau)\right] - \sin(\omega_0 \tau)\cos(\omega_0 t_0)\right]^2 \\
&= \frac{1}{2}\frac{e^2E_0^2}{m\omega_0^2}\left[\cos(\omega_0 t_0)\tan(\omega_0 t_0)\left[1 - \cos(\omega_0 \tau)\right] - \sin(\omega_0 \tau)\cos(\omega_0 t_0)\right]^2
\end{aligned}$$

Here we can insert equation # in the above equation and we get

$$E_k = \frac{1}{2}\frac{e^2E_0^2}{m\omega_0^2}\left[\cos(\omega_0 t_0)\frac{\left[\cos(\omega_0\tau)-1\right]}{\left[\sin(\omega_0\tau)-\tau\omega_0\right]}\left[1-\cos(\omega_0\tau)\right]-\sin(\omega_0\tau)\cos(\omega_0 t_0)\right]^2$$

$$= \frac{1}{2}\frac{e^2E_0^2}{m\omega_0^2}\cos^2(\omega_0 t_0)\left[\frac{-\cos^2(\omega_0\tau)-1+2\cos(\omega_0\tau)}{\left[\sin(\omega_0\tau)-\tau\omega_0\right]}-\sin(\omega_0\tau)\right]^2$$

$$= \frac{1}{2}\frac{e^2E_0^2}{m\omega_0^2}\cos^2(\omega_0 t_0)\left[\frac{-\cos^2(\omega_0\tau)-1+2\cos(\omega_0\tau)-\sin^2(\omega_0\tau)+\tau\omega_0\sin(\omega_0\tau)}{\left[\sin(\omega_0\tau)-\tau\omega_0\right]}\right]^2$$

$$= \frac{1}{2}\frac{e^2E_0^2}{m\omega_0^2}\cos^2(\omega_0 t_0)\left[\frac{-\left[\cos^2(\omega_0\tau)+\sin^2(\omega_0\tau)\right]-1+2\cos(\omega_0\tau)+\tau\omega_0\sin(\omega_0\tau)}{\left[\sin(\omega_0\tau)-\tau\omega_0\right]}\right]^2$$

$$= \frac{1}{2}\frac{e^2E_0^2}{m\omega_0^2}\cos^2(\omega_0 t_0)\left[\frac{-1-1+2\cos(\omega_0\tau)+\tau\omega_0\sin(\omega_0\tau)}{\left[\sin(\omega_0\tau)-\tau\omega_0\right]}\right]^2$$

$$= \frac{1}{2}\frac{e^2E_0^2}{m\omega_0^2}\cos^2(\omega_0 t_0)\left[\frac{-2+2\cos(\omega_0\tau)+\tau\omega_0\sin(\omega_0\tau)}{\left[\sin(\omega_0\tau)-\tau\omega_0\right]}\right]^2$$

Now, using trigonometric identity for $\cos(2\omega_0 t_0)$, we can write:

$$\cos(2\omega_0 t_0) = \frac{1-\tan^2(\omega_0 t_0)}{1+\tan^2(\omega_0 t_0)} = \frac{1-\left[\dfrac{\cos(\omega_0\tau)-1}{\sin(\omega_0\tau)-\tau\omega_0}\right]^2}{1+\left[\dfrac{\cos(\omega_0\tau)-1}{\sin(\omega_0\tau)-\tau\omega_0}\right]^2}$$, using equation #.

$$\text{or, } \cos(2\omega_0 t_0) = \frac{\dfrac{\left[\sin(\omega_0\tau)-\tau\omega_0\right]^2-\left[\cos(\omega_0\tau)-1\right]^2}{\left[\sin(\omega_0\tau)-\tau\omega_0\right]^2}}{\dfrac{\left[\sin(\omega_0\tau)-\tau\omega_0\right]^2+\left[\cos(\omega_0\tau)-1\right]^2}{\left[\sin(\omega_0\tau)-\tau\omega_0\right]^2}} = \frac{\left[\sin(\omega_0\tau)-\tau\omega_0\right]^2-\left[\cos(\omega_0\tau)-1\right]^2}{\left[\sin(\omega_0\tau)-\tau\omega_0\right]^2+\left[\cos(\omega_0\tau)-1\right]^2}$$

Now, as $\cos^2(\omega_0 t_0) = \dfrac{1+\cos(2\omega_0 t_0)}{2}$, we can write

$$\cos^2(\omega_0 t_0) = \frac{1+\frac{\left[\sin(\omega_0\tau)-\tau\omega_0\right]^2-\left[\cos(\omega_0\tau)-1\right]^2}{\left[\sin(\omega_0\tau)-\tau\omega_0\right]^2+\left[\cos(\omega_0\tau)-1\right]^2}}{2}$$

$$= \frac{1}{2}\frac{\left[\sin(\omega_0\tau)-\tau\omega_0\right]^2+\left[\cos(\omega_0\tau)-1\right]^2+\left[\sin(\omega_0\tau)-\tau\omega_0\right]^2-\left[\cos(\omega_0\tau)-1\right]^2}{\left[\sin(\omega_0\tau)-\tau\omega_0\right]^2+\left[\cos(\omega_0\tau)-1\right]^2}$$

$$= \frac{\left[\sin(\omega_0\tau)-\tau\omega_0\right]^2}{\left[\sin(\omega_0\tau)-\tau\omega_0\right]^2+\left[\cos(\omega_0\tau)-1\right]^2}$$

Inserting equation # in equation #, we get

$$E_k = \frac{1}{2}\frac{e^2E_0^2}{m\omega_0^2}\frac{\left[\sin(\omega_0\tau)-\tau\omega_0\right]^2}{\left[\sin(\omega_0\tau)-\tau\omega_0\right]^2+\left[\cos(\omega_0\tau)-1\right]^2}\left[\frac{-2+2\cos(\omega_0\tau)+\tau\omega_0\sin(\omega_0\tau)}{\left[\sin(\omega_0\tau)-\tau\omega_0\right]}\right]^2$$

$$= \frac{1}{2}\frac{e^2E_0^2}{m\omega_0^2}\frac{\left[2-2\cos(\omega_0\tau)-\tau\omega_0\sin(\omega_0\tau)\right]^2}{\left[\sin(\omega_0\tau)-\tau\omega_0\right]^2+\left[\cos(\omega_0\tau)-1\right]^2}$$

$$= \frac{1}{2}\frac{e^2E_0^2}{m\omega_0^2}\frac{\left[2-2\cos(\omega_0\tau)-\tau\omega_0\sin(\omega_0\tau)\right]^2}{\sin^2(\omega_0\tau)-2\tau\omega_0\sin(\omega_0\tau)+\tau^2\omega_0^2+\cos^2(\omega_0\tau)-2\cos(\omega_0\tau)+1}$$

$$= \frac{1}{2}\frac{e^2E_0^2}{m\omega_0^2}\frac{\left[2-2\cos(\omega_0\tau)-\tau\omega_0\sin(\omega_0\tau)\right]^2}{\left[1-2\tau\omega_0\sin(\omega_0\tau)+\tau^2\omega_0^2-2\cos(\omega_0\tau)+1\right]}$$

$$= \frac{1}{2}\frac{e^2E_0^2}{m\omega_0^2}\frac{\left[2-2\cos(\omega_0\tau)-\tau\omega_0\sin(\omega_0\tau)\right]^2}{\left[2-2\tau\omega_0\sin(\omega_0\tau)+\tau^2\omega_0^2-2\cos(\omega_0\tau)\right]}$$

Thus, the above equation suggests that the final kinetic energy of the electron due to acceleration and recombination depends on total time taken due to acceleration and recombination. Now let us derive an expression for the Ponderomotive energy (U_p), which is defined as the average kinetic energy gained by the electron over on optical cycle if the electron was assumed to be at rest in an atom (i.e., $\mathrm{v}_0 = 0$):

$$U_p = \frac{1}{2}m\frac{1}{T}\int_{t-T/2}^{t+T/2}\left[\mathrm{v(t)}\right]^2 dt$$

$$= \frac{1}{2}\frac{e^2E_0^2}{m\omega_0^2}\frac{1}{T}\int_{t-T/2}^{t+T/2}\sin^2(\omega_0 t)dt = \frac{1}{2}\frac{e^2E_0^2}{m\omega_0^2}\frac{1}{2} = \frac{1}{4}\frac{e^2E_0^2}{m\omega_0^2}$$

Here we have used standard integral $\frac{1}{T}\int_{t-T/2}^{t+T/2}\sin^2(\omega_0 t)dt=\frac{1}{2}$. Substituting equation # for U_p, we get $E_k=2U_p\frac{\left[2-2\cos(\omega_0\tau)-\tau\omega_0\sin(\omega_0\tau)\right]^2}{\left[2-2\tau\omega_0\sin(\omega_0\tau)+\tau^2\omega_0^2-2\cos(\omega_0\tau)\right]}$. Figure # shows a plot of E_k/U_p as a function of $\omega_0\tau$, which shows a maximum at $\frac{E_k^{MAX}}{U_p}=3.17$, which estimates the maximum kinetic energy of the electron which can be given as $E_k=3.17U_p$. Thus, the cut-off energy becomes $\left(I_p+3.17U_p\right)$.

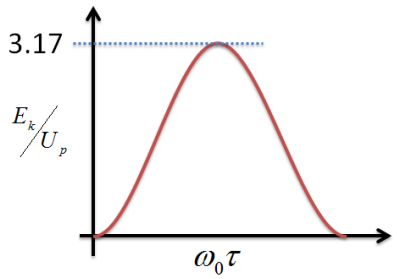

Figure #: Plot of E_k/U_p vs $\omega_0\tau$.

Phase matching in HHG:

Studying the HHG process in a single atom response model (i.e., three step model, given above) basically provides the predicted shape of the harmonic spectrum. However, it cannot account for other observed harmonic yield. To obtain strong harmonic emission (increase the efficiency of frequency up-conversion process in HHG), phase matching conditions also need to be considered. A useful introduction to phase matching conditions is given in this chapter in the context of SHG, which highlights that to produce optical harmonics efficiently, the process must be phase-matched, i.e., the fundamental beam or induced polarization and harmonic beam must be brought in phase through-out the nonlinear medium. Furthermore, we have seen that intensity of the harmonic emission is given by (if the medium is not absorbing the harmonic beam, i.e., for loss-less medium):

$$I(L,t)=\frac{\mu_0^2\omega_0^4}{4k_0^2}\left|b(z,t)\right|^2 L^2\frac{sin^2\left(\frac{\Delta kL}{2}\right)}{\left(\frac{\Delta kL}{2}\right)^2},$$

where, L is the distance transmitted in the medium. This equation shows that harmonic intensity varies as $\frac{sin^2\left(\frac{\Delta kL}{2}\right)}{\left(\frac{\Delta kL}{2}\right)^2}$ or $\text{sinc}^2\left(\frac{\Delta kL}{2}\right)$ and it will be maximum at a distance $L_c = \frac{\pi}{\Delta k}$, which is known as the coherence length.

Now let us take an example of second harmonic generation (SHG) again. Suppose that we wish to frequency-double a wavelength of $1\,\mu m$ to a wavelength of $500nm$ using a KDP crystal as the nonlinear medium. For this SHG, $L_c = \frac{\pi}{\Delta k} = \frac{\pi}{k_0 - k_p} = \frac{\lambda}{4\left[n\left(\frac{\lambda}{2}\right) - n(\lambda)\right]}$. Here, $\lambda = 1\mu m$, $n(500nm) = 1.529833$, and $n(1\mu m) = 1.50873$. Thus, $L_c = 11.8\mu m$. Most nonlinear medium exhibits similar coherence lengths, even it is true for HHG. This suggests that as Δk approaches zero, the harmonic signal will grow proportionallyto L^2. But, as it is true for all other non-linear frequency conversion processes, phase matching in HHG is not easily achieved.

The phase mismatch Δk for the HHG process can be written as

$$\Delta k_q = k_o^q - k_p = k_o^q - qk_1,$$

where, q is the harmonic order, k_o^q is the wave vector of the q th harmonic and k_1 is the wave vector of the fundamental (input) beam. For a partially ionized gas medium the refractive index can be written as, $n = 1 + P\left[(1-\eta)n(\lambda) - \eta N_{atm} r_e \frac{\lambda^2}{2\pi} + (1-\eta)n_2 I\right]$,where, P is the pressure in atmosphere, η is the ionization fraction, N_{atm} is number density at one atmosphere, $n(\lambda)$ is refractive index of neutral atoms at λ per unit pressure.Thus, the propagation vector can be written as

$$k = \frac{2\pi}{\lambda} n = \frac{2\pi}{\lambda}\left[1 + P(1-\eta)n(\lambda) - P\eta N_{atm} r_e \frac{\lambda^2}{2\pi} + P(1-\eta)n_2 I\right]$$
$$= \frac{2\pi}{\lambda} + \frac{2\pi P(1-\eta)n(\lambda)}{\lambda} - P\eta N_{atm} r_e \lambda + \frac{2\pi}{\lambda} P(1-\eta)n_2 I$$

Here, four terms on the right hand side correspond to vacuum contribution, contribution of neutral gas dispersion, plasma dispersion, and nonlinear refractive index, respectively. For partially ionized gas medium confined inside a waveguide, additional dispersion term due to waveguide is also included and magnitude of propagation vector is written as

$$k = \frac{2\pi}{\lambda} + \frac{2\pi P(1-\eta)n(\lambda)}{\lambda} - P\eta N_{atm} r_e \lambda + \frac{2\pi}{\lambda} P(1-\eta) n_2 I - \frac{\mu_{mn}^2 \lambda}{4\pi a^2},$$

where, a is the inner radius of the waveguide, μ_{mn} is root of Bessel function, corresponding to the waveguide mode. For gas jet created due to supersonic jet expansion, equation # is considered for the expression of k. However, for general derivation of phase mismatch (Δk_q), we shall consider waveguide contribution as well.

Thus, can now calculate the phase mismatch:

$$\begin{aligned}\Delta k_q &= k_o^q - q k_1 \\ &= \left[\frac{2\pi}{\lambda_0} + \frac{2\pi P(1-\eta)n(\lambda)}{\lambda_0} - P\eta N_{atm} r_e \lambda_0 + \frac{2\pi}{\lambda_0} P(1-\eta) n_2 I - \frac{\mu_{mn}^2 \lambda_0}{4\pi a^2}\mu_{mn}\right] - \\ &\qquad \left[\frac{2\pi}{\lambda_1} + \frac{2\pi P(1-\eta)n(\lambda)}{\lambda_1} - P\eta N_{atm} r_e \lambda_1 + \frac{2\pi}{\lambda_1} P(1-\eta) n_2 I - \frac{\mu_{mn}^2 \lambda_1}{4\pi a^2}\mu_{mn}\right]\end{aligned}$$

Here $\lambda_0 = \frac{\lambda_1}{q}$. Thus, we get,

$$\begin{aligned}\Delta k_q &= \left[\frac{2\pi q}{\lambda_1} + \frac{2\pi q P(1-\eta)n(\lambda)}{\lambda_1} - P\eta N_{atm} r_e \frac{\lambda_1}{q} + \frac{2\pi q}{\lambda_1} P(1-\eta) n_2 I - \frac{\mu_{mn}^2 \lambda_1}{4\pi q a^2}\mu_{mn}\right] - \\ &\qquad \left[\frac{2\pi}{\lambda_1} + \frac{2\pi P(1-\eta)n(\lambda)}{\lambda_1} - P\eta N_{atm} r_e \lambda_1 + \frac{2\pi}{\lambda_1} P(1-\eta) n_2 I - \frac{\mu_{mn}^2 \lambda_1}{4\pi a^2}\mu_{mn}\right]\end{aligned}$$

or, $\Delta k_q = \frac{2\pi q P(1-\eta)}{\lambda_1}\left[n\left(\frac{\lambda_1}{q}\right) - n(\lambda_1)\right] - P\eta N_{atm} r_e \lambda_1 \left[\frac{1}{q} - q\right] - \frac{\mu_{mn}^2 \lambda_1}{4\pi a^2}\left[\frac{1}{q} - q\right]$

Thus, phase matching of HHG can be can be achieved ($\Delta k_q = 0$) by balancing various parameters given in the above equation, including pressure, ionization fraction, μ_{mn} (This comes in case of waveguide, which is a physical quantity related to modes of waveguide).

Let us now take a closer look at those factors which contribute to the phase mismatch because the harmonic yield is severely affected by phase mismatch. The first term on the right hand side of the equation # arises due phase mismatch caused by neutral gas dispersion, which depends on pressure, difference of the refractive indices at the fundamental and harmonic wavelengths and ionization fraction. Ionization fraction (which determines the ratio of neutral atoms and ionized atoms) solely depends on the intensity of the fundamental laser beam. Note that neutral gas dispersion is positive.

The second term arises due to phase mismatch contributed by plasma dispersion, which is negative. When an intense laser beam interacts with a gas medium, free electrons are emitted. These free electrons cause plasma dispersion. As the contribution from the phase mismatch due to neutral gas dispersion is positive and that due to plasma dispersion is negative, the total phase mismatch (Δk_q) can be reduced by varying the laser intensity to adjust the ionization fraction (η). Considering gas jet (excluding waveguide contribution), for phase matched condition (i.e., when phase mismatch due to neutral gas dispersion is fully compensated by that due to plasma dispersion),

$$\Delta k_q = 0 = \frac{2\pi q P(1-\eta)}{\lambda_1}\left[n\left(\frac{\lambda_1}{q}\right) - n(\lambda_1)\right] - P\eta N_{atm} r_e \lambda_1 \left[\frac{1}{q} - q\right]$$

$$\text{or, } \frac{2\pi q P(1-\eta_c)}{\lambda_1}\left[n\left(\frac{\lambda_1}{q}\right) - n(\lambda_1)\right] = P\eta_c N_{atm} r_e \lambda_1 \left[\frac{1}{q} - q\right]$$

$$\text{or, } \frac{(1-\eta_c)}{\eta_c} = \frac{N_{atm} r_e \lambda_1^2 \left[\frac{1}{q^2} - 1\right]}{2\pi\Delta n}, \text{ where } \Delta n = \left[n\left(\frac{\lambda_1}{q}\right) - n(\lambda_1)\right]$$

$$\text{or, } \frac{1}{\eta_c} = \left[1 + \frac{N_{atm} r_e \lambda_1^2 \left[\frac{1}{q^2} - 1\right]}{2\pi\Delta n}\right]$$

$$\text{or, } \eta_c = \left[1 + \frac{N_{atm} r_e \lambda_1^2 \left[\frac{1}{q^2} - 1\right]}{2\pi\Delta n}\right]^{-1}$$

Here, for harmonic generation (in VUV, XUV and soft X-ray regimes) $\Delta n = n(XUV) - n(800nm)$ is always negative, as schematically illustrated in Figure 8. η_c in the above equation features critical ionization fraction above which dispersion from the remaining neutral atoms is not enough to balance the dispersion from the plasma. Hence, in order to obtain phase matching in HHG, ionization fraction must be equal to critical ionization fraction. Note that critical ionization fraction does not depend on gas pressure. Typical values for critical ionization fraction for common gases at 800 nm are quite low, about 0.5% in He, 1% Ne, and 5% in Ar. Furthermore, there is an upper limit of the input laser intensity for HHG. At intensity above 10^{16} w/cm^2 the increased magnetic field prevents recombination step in HHG process,

which is discussed later in this section. Self-focusing and creation of optically opaque plasma are also limiting factors at this intensity.

In addition to the factors discussed above, another two factors also contribute to phase matching:

Geometric phase mismatch: When a Gaussian laser beam is focused, geometrical phase shifts by π around the focal point: this is called Gouy phase shift, which is discussed in Chapter #. This leads to a phase mismatch between the fundamental beam and the emitted XUV beam. In order to overcome this, the focus in the gas jet needs to be placed before the HHG medium which leads to efficient spatial and spectral harmonics. If the focus is placed at the centre of the medium, the harmonic intensity becomes low, owing to poor phase matching.

Re-absorption of harmonic emission: Even if the phase matching is achieved, the conversion efficiency in HHG process is still limited by re-absorption of the harmonic emission in the HHG medium. For phase matched harmonic emission, coherent harmonic signal intensity grows with the interaction length (L^2) and with increasing gas pressure. Then the harmonic beam travels through an absorbing medium and with no new harmonic generation, the signal is also attenuated in propagation to the negative exponential of the medium length and gas pressure. Thus, harmonic yield approach the maximum value for a particular interaction length and gas pressure. This is called absorption limit, which also limits the total harmonic generation efficiency.

(

Chapter 3: TDSE

Highlights:

Introduction:

Understanding attosecond phenomena requires solution of the time-dependent Schrödinger equation (TDSE). This is why, in this chapter, we first shall go over the TDSE for general laser-matter interactions and review approaches to numerically solve the TDSE for atomic and molecular systems in strong laser fields.

High harmonic generation (HHG) represents an extreme nonlinear process, in which more than 10 or even 100 input photons from a visible or near infrared (NIR) laser are combined together